

# Improvement of Single-Crystal Structures of Very Heavy Element Compounds by Refining Anomalous Dispersion Parameters

Florian Meurer, Gregory Morrison, Birgit Hischa, Hans-Conrad zur Loye, Christoph Hennig,\* and Michael Bodensteiner\*



Cite This: *Inorg. Chem.* 2024, 63, 15784–15790



Read Online

ACCESS |



Metrics & More

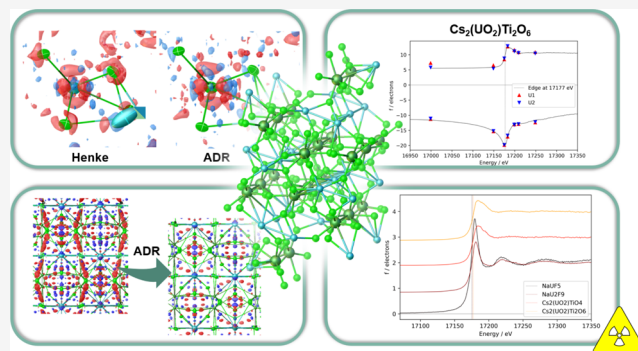


Article Recommendations



Supporting Information

**ABSTRACT:** Refining the anomalous dispersion parameters of the four uranium compounds  $\text{NaUF}_5$ ,  $\text{NaU}_2\text{F}_9$ ,  $\text{Cs}_2(\text{UO}_2)\text{TiO}_4$ , and  $\text{Cs}_2(\text{UO}_2)\text{Ti}_2\text{O}_6$  gave insights into the crystallographic model improvement of very heavy atoms. We found that the values for the dispersive and absorptive parts,  $f'$  and  $f''$ , closely followed the X-ray absorption spectra on their  $L_3$ ,  $L_2$ , and  $L_1$  edges. The obtained values are sensitive to the chemical environment at each crystallographically independent position. An incorrect treatment of the anomalous dispersion correction can lead to a wrong crystallographic model. The above-mentioned, already published structures were improved by this process. General guidelines were given for the crystal structure determination of very heavy compounds. When using Mo  $K\alpha$  radiation with uranium compounds, the proximity of its energy to the uranium L-edges causes a noticeable effect.



## INTRODUCTION

In single-crystal X-ray diffraction (SC-XRD), the anomalous dispersion terms  $f'$  and  $f''$  correct for the nonelastic behavior of a given element. They correspond directly to an X-ray absorption spectrum (XAS) and its Kramers–Kronig transformation (KKT), which contain valuable chemical information when recorded over several energies near the absorption edge of an element.<sup>1,2</sup> In protein crystallography, this relation has been shown to provide valuable spatially resolved chemical information in important systems such as nitrogenase FeMoco and the FeV cofactor.<sup>3–5</sup> It has received much less attention for small-molecule SC-XRD, with rare examples being presented, for instance, by Bartholomew et al.<sup>6,7</sup> This is surprising as the initial research into the refinement of the anomalous dispersion correction terms goes back as early as 1978 and was well examined by L. K. Templeton and D. H. Templeton.<sup>8,9</sup>

In 2022, we have described the application and implementation of anomalous dispersion refinement (ADR) within one of the most widely used crystallographic software suites Olex2.<sup>10</sup> In this work, a good agreement was found between a recorded X-ray absorption spectrum (XAS) of the organometallic compound  $\text{Mo}(\text{CO})_6$  and its KKT with the refined values for  $f''$  and  $f'$  obtained directly from the diffraction data.

Most recently, Leinders et al. published their investigations on ADR of tetravalent uranium dioxide as well as pentavalent  $\text{KUO}_3$  with powder diffraction.<sup>11</sup> In this study, the dispersive part of the atomic form factor  $f'$  was obtained by the

transformation of refined  $f''$  values and introduced as a parameter in the least-squares refinement procedure. In contrast, we refined both  $f'$  and  $f''$  for uranium directly from the experimental intensities from single-crystal data.

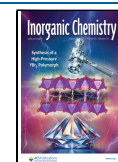
Uranium-containing compounds are interesting both chemically and crystallographically. Their chemistry has been and continues to be extensively studied, especially in the context of nuclear waste deposits.<sup>12</sup> The different oxidation states and bonding motifs of uranium make it interesting from a crystal chemistry viewpoint. In oxides, the +6 oxidation state is most prominent, and U(VI) almost always forms the uranyl cation,  $\text{UO}_2^{2+}$ , which consists of a central uranium atom strongly bound to two oxygens with an almost  $180^\circ$  arrangement. The uranyl uranium is further coordinated by four, five, or six equatorial oxygens to form square, pentagonal, or hexagonal bipyramids.<sup>13</sup> The two strongly coordinated uranyl oxygens rarely participate in further bonding<sup>14</sup> except to weakly bond to low valent cations such as the alkali cations.<sup>15,16</sup> For this reason, the uranyl ion promotes the formation of layered and channel structures. In fluorides, uranium often adopts the +4

**Received:** April 29, 2024

**Revised:** July 24, 2024

**Accepted:** July 30, 2024

**Published:** August 8, 2024



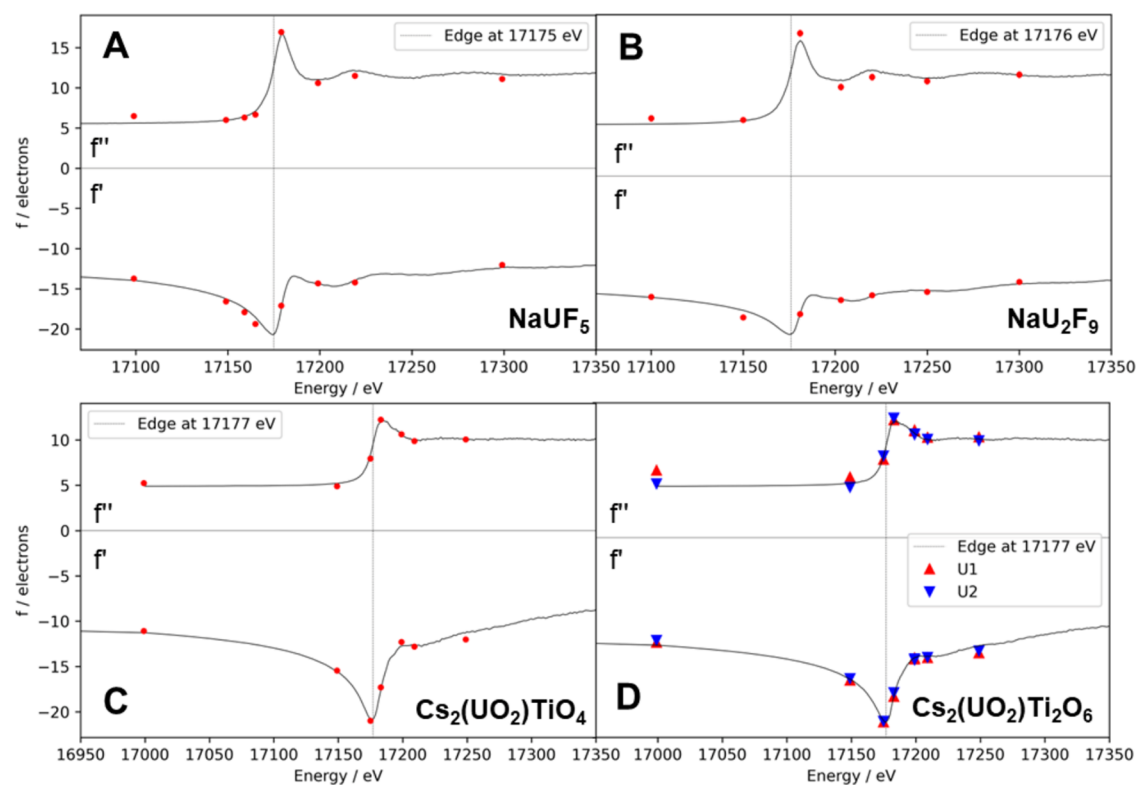


**Figure 1.** Each plot shows the recorded XAS (top) and its KKT (bottom) for the  $L_3$  edge of uranium in four different compounds, together with the freely refined values for  $f''$  and  $f'$  from SC-XRD data at different energies. Absorption edges, determined from the strongest maximum in the first derivative of the XAS, are also given (vertical gray lines). The XAS and its KKT were first normalized and then fitted to the ADR parameters.

oxidation state and typically forms irregular 8- or 9-coordinate polyhedra.<sup>13,17,18</sup>

Crystallographically, uranium typically exhibits a large residual electron density in its vicinity, a common problem with very heavy elements. Particularly for these elements, the values for anomalous dispersion correction can become quite large. For example, when uranium compounds are measured using Mo  $K\alpha$  radiation ( $E = 17.4$  keV), just above the uranium  $L_3$  absorption edge ( $E = 17.1$  keV), a significant fraction of the incoming radiation is absorbed and dispersed ( $f' = -10.2$  e,  $f'' = 10.4$  e according to Henke et al.<sup>19</sup>). As the atomic scattering power is closely connected to the atomic position, displacement parameters, and most notably the element type, an adequate correction for these effects is essential for determining the correct structure. The quality of the structural model strongly depends on the treatment of these effects.

Herein, we present the capability and robustness of anomalous dispersion refinements (ADR) carried out at the L absorption edges of the known uranium single-crystalline compounds  $\text{NaUF}_5$ ,  $\text{NaU}_2\text{F}_9$ ,  $\text{Cs}_2(\text{UO}_2)\text{TiO}_4$ , and  $\text{Cs}_2(\text{UO}_2)\text{Ti}_2\text{O}_6$ .<sup>18,20</sup> ADR was able to capture the features within the strongly pronounced  $L_3$  edge of these compounds as well as the weaker  $L_2$  and  $L_1$  edges. For  $\text{NaUF}_5$ , we present the dependency of ADR at room temperature (RT) as well as at 100 K. As ADR introduces two additional variables per resonating atom to the crystallographic model, it is important to investigate to what extent ADR improves the residual electron density and whether the correction parameters compensate for other effects.

## METHODS

To investigate the behavior of ADR at heavy element L-edges, SC-XRD experiments were performed at various energies around the uranium L-edges ( $L_3$ : 17.166 keV,  $L_2$ : 20.948 keV,  $L_1$ : 21.757 keV<sup>21</sup>). Simultaneously, X-ray absorption spectra were recorded on the same single crystals in fluorescence mode in the range of these energies. All experiments were performed at the Rossendorf Beamline (BM20) at the European Synchrotron (ESRF) in Grenoble, France.<sup>22</sup>

X-ray diffraction data were processed in CrysAlisPro<sup>23</sup> and evaluated in Olex2<sup>24</sup> using olex2.refine<sup>25</sup> as a refinement engine employing the serial processing module SISYPHOS.<sup>26</sup> All data were treated with only multiscan absorption correction<sup>27</sup> to avoid including the linear absorption coefficient  $\mu$ . This is due to the direct proportionality between  $\mu$  and  $f''$ , the absorbing part of the dispersion correction. Especially in the edge region, the tabulated values are the most incorrect, as both the edge position and the fine structure features are individuals for each substance. Therefore, any absorption correction based on  $\mu$  is also incorrect, particularly in this area.

XAS data were processed using the PyMCA<sup>28</sup> software suite, and the Kramers–Kronig transformations were performed using the kkalcc<sup>29</sup> program. Further details can be found in the Supporting Information (SI).

## RESULTS AND DISCUSSION

The results from ADR together with the recorded U  $L_3$  edge XAS data in both uranium(IV) fluorides and uranyl titanates are shown in Figure 1. In all cases, we observed good agreement between the XAS/KKT and the independently refined values for  $f''/f'$  obtained from SC-XRD data. The absolute values for  $f'$  and  $f''$  follow the fine structure in the near edge region of XAS. The two crystallographically independent positions for uranium in  $\text{Cs}_2(\text{UO}_2)\text{Ti}_2\text{O}_6$  (Figure 1D) are chemically equivalent. This was reflected by very

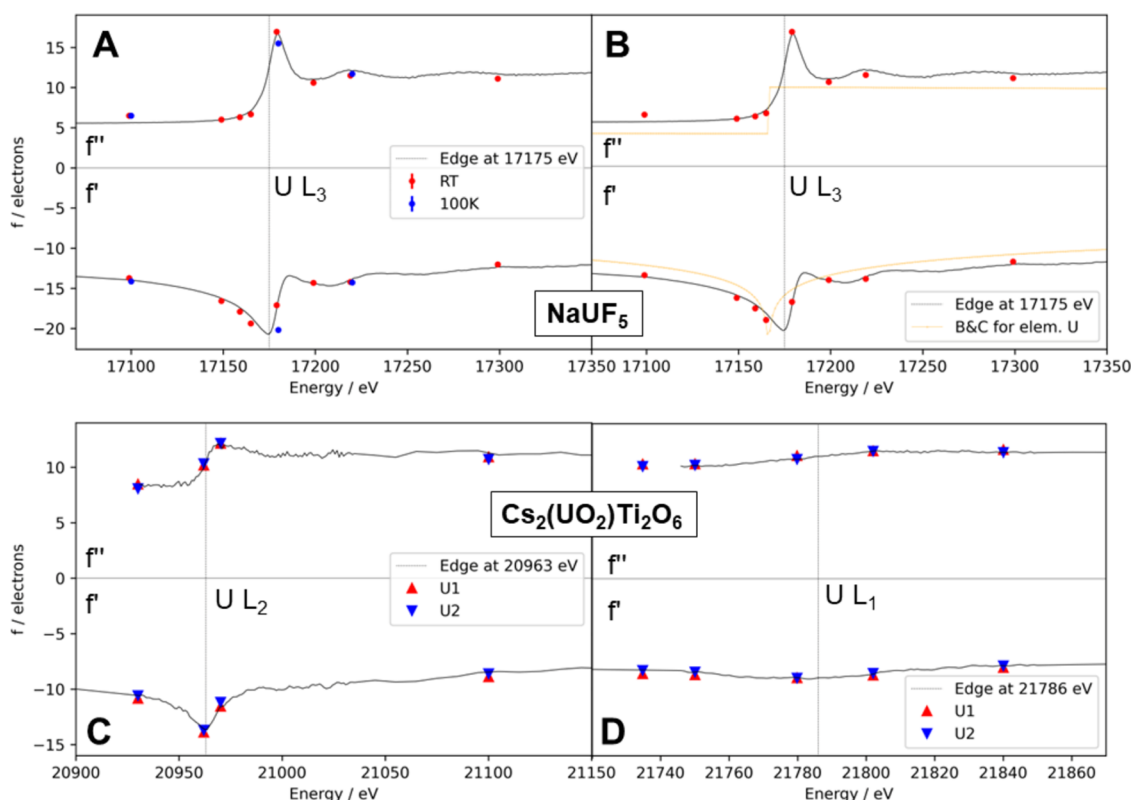


**Figure 2.** Each plot shows the recorded XAS (top) and its KKT (bottom) for  $\text{NaUF}_5$  (A, B) and  $\text{Cs}_2(\text{UO}_2)\text{Ti}_2\text{O}_6$  (C, D), together with the freely refined values for  $f''$  (top) and  $f'$  (bottom) from XRD data at the different energies. A shows the ADR parameters at room temperature (red) as well as at 100 K (blue). (B) shows the values compared to the calculated values for uranium according to Brennan and Cowan.<sup>30</sup> Panels (C) and (D) compare the spectra to ADR values at the  $\text{U L}_2$  and  $\text{U L}_1$  absorption edge, respectively. The XAS and its KKT were first normalized and then fitted to the ADR parameters.

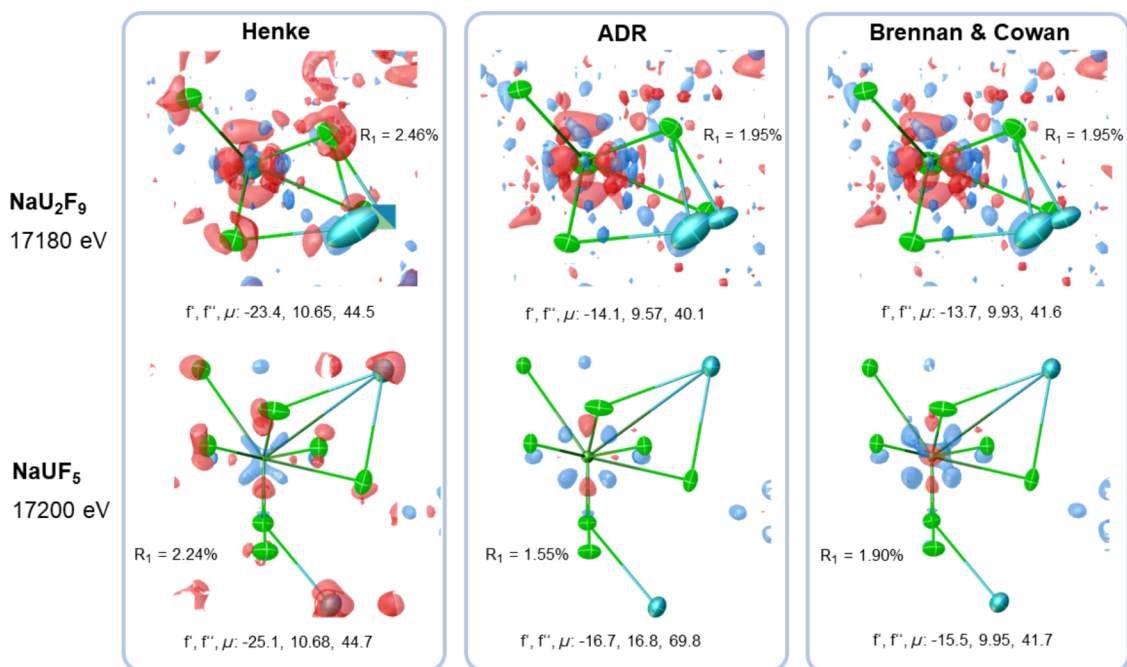


**Figure 3.** Residual electron density maps (blue: positive, red: negative) for the asymmetric units of  $\text{NaU}_2\text{F}_9$  (top,  $1.0 \text{ e} \cdot \text{\AA}^{-3}$  iso-surface) and  $\text{NaUF}_5$  (bottom,  $0.9 \text{ e} \cdot \text{\AA}^{-3}$  iso-surface) modeled according to Henke<sup>19</sup> (left, linearly interpolated), ADR (middle), and Brennan and Cowan<sup>30</sup> (right, calculated). Ellipsoids are shown at 50% probability level, and tetrahedra indicate nonpositive definite displacement parameters.  $f'$  and  $f''$  values are given in electrons and elemental  $\mu$  in kilobarns per atom.



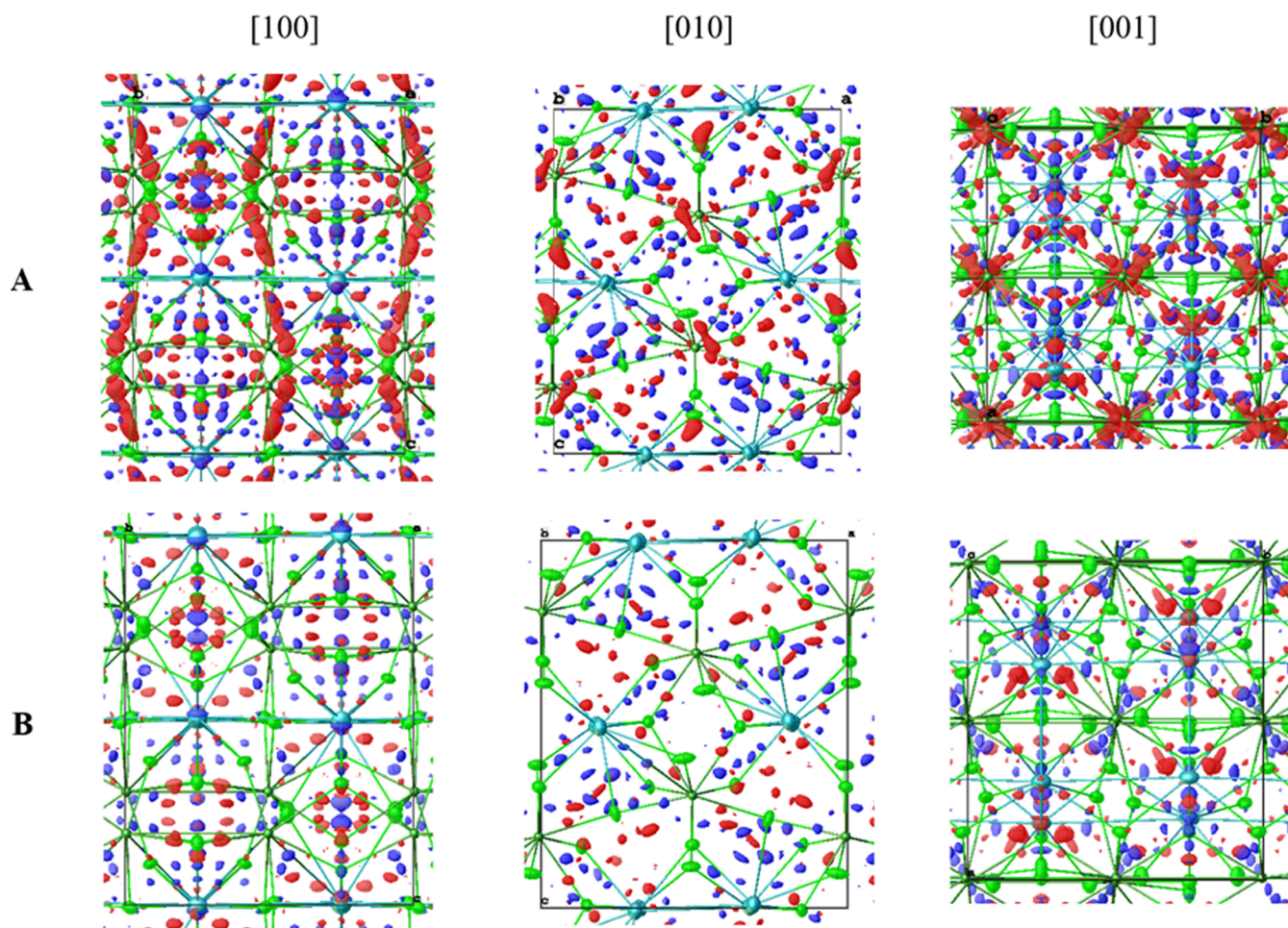


**Figure 4.** Residual electron density maps at  $0.6 \text{ e}\cdot\text{\AA}^{-3}$  iso-level (blue: positive, red: negative) for the structure of  $\text{NaUF}_5$  (CCDC 1827659)<sup>18</sup> refined as published using Henke (A) and refined anomalous dispersion values (B) in crystallographic  $a$ ,  $b$ , and  $c$  directions. Light green atoms: fluorine, dark green atoms: uranium, and cyan atoms: sodium.

similar ADR values and underlined the sensitivity of ADR toward chemical features.

Figure 2 shows a good agreement between  $f'$  and  $f''$  and no significant temperature dependence for ADR of  $\text{NaUF}_5$  at two temperatures (RT and 100 K, A). Only at the edge energy, a deviation was observed. However, this difference could be due to a small energy difference that can occur when the synchrotron beam is readjusted. For technical reasons, the low-temperature measurements were not carried out directly after the room-temperature experiments. Especially in the absorption edge, such a rather small drift in energy can already lead to a considerable deviation in absorption.

Most prominently, a large difference was observed between the refined  $f'$  and  $f''$  values compared to the calculated dispersion correction according to Brennan and Cowan (Figure 2, B).<sup>30</sup> Not only was there a typical offset due to the difference in edge energy between elemental uranium and uranium embedded in a chemical environment (here by 9 eV), but there was also a shift to higher absolute values for  $f'$  and  $f''$ . This trend was also observed for the other compounds of this study (see Figure S4 in the SI). Furthermore, a good agreement was also found at the less pronounced  $L_2$  and  $L_1$  edges in the respective spectra and even for the two uranium positions in the case of  $\text{Cs}_2(\text{UO}_2)\text{Ti}_2\text{O}_6$ .

In Figure 3, the residual electron density maps show the crystallographic models for three different sources of

anomalous dispersion corrections above the absorption edge of uranium. In the case of  $\text{NaU}_2\text{F}_9$ , a significant difference between the model relying on the Henke table<sup>19</sup> and the one for Brennan and Cowan<sup>30</sup> was apparent. Using Henke the agreement strongly decreased and a disorder in the sodium position, far away from the uranium atom, could not be modeled properly. The values obtained from ADR closely matched those of Brennan and Cowan,<sup>30</sup> and similar agreement was obtained between measured and modeled structure factors as indicated by the crystallographic  $R_1$  value.

In the case of  $\text{NaUF}_5$ , ADR showed a better agreement with the measured data compared to the models using the values from Henke<sup>19</sup> and Brennan and Cowan.<sup>30</sup> This suggests that ADR provided the most accurate values for anomalous dispersion correction in this approach, especially where pronounced spectral features dominate the XAS.

Generally, Brennan and Cowan<sup>30</sup> gave a good approximation, except for the edge region. This was particularly relevant for uranium compounds measured with Mo  $K\alpha$  radiation ( $E_{\text{Mo } K\alpha} = 17.4 \text{ keV}$ ), which lies just above the U  $L_3$  edge. This was reflected very well in the work of Gianopoulos et al.,<sup>31</sup> where in a charge density study of uranium, the anomalous dispersion values refined very close to those calculated by Brennan and Cowan.<sup>30</sup>

Note that the resulting elemental absorption coefficient for uranium differed by more than 50% (69.8 kilobarns per atom

**Table 1.** Refinement indicators achieved with the Brennan and Cowan<sup>30</sup> (B&C) anomalous dispersion values as well as by ADR for the published data of the four compounds within this study<sup>a,18,20</sup>

	NaUF <sub>5</sub>		NaU <sub>2</sub> F <sub>9</sub>		Cs <sub>2</sub> (UO <sub>2</sub> )TiO <sub>4</sub>		Cs <sub>2</sub> (UO <sub>2</sub> )Ti <sub>2</sub> O <sub>6</sub>	
	B&C	ADR	B&C	ADR	B&C	ADR	B&C	ADR
<i>R</i> <sub>1</sub> , w <i>R</i> <sub>2</sub> /%	1.32, 2.64	1.26, 2.50	1.34, 3.07	1.33, 2.98	1.12, 2.52	1.08, 2.42	1.20, 2.87	1.08, 2.51
min., max. peaks/e·Å <sup>-3</sup>	-0.93, 1.07	-0.97, 0.97	-0.89, 1.11	-0.89, 1.03	-0.74, 0.73	-0.62, 0.67	-0.86, 1.67	-0.935, 1.53
weights	0.00, 2.91	0.00, 1.92	0.01, 0.87	0.01, 0.53	0.01, 21.0	0.00, 19.2	0.01, 11.7	0.01, 2.39
<i>f</i> ' , <i>f</i> ''/e	-9.7, 9.7	-11.9(3), 11.8(6)	-9.7, 9.7	-11.1(3), 9.9(6)	-9.7, 9.7	-10.2(4), 10.5(8)	-9.7, 9.7	-10.5, -11.3, 10.2, 10.1

<sup>a</sup>The published structures were re-refined using *olex2.refine*<sup>25</sup> employing the recently published improved spherical model according to Thakkar.<sup>32,33</sup> Additionally, for the uranyl titanate structures, the cesium atoms were refined anharmonically. Quality parameters were calculated to a resolution of 0.75 Å, and *f*' and *f*'' were refined at the maximum resolution of the dataset.

with ADR, 41.7 kilobarns per atom according to Brennan and Cowan<sup>30</sup>). Such a difference can have a significant effect on the analytical absorption correction, which is essential for atomic structures containing heavy elements. Since *f*'' and  $\mu$  are directly proportional to each other, their dependence is obvious. However,  $\mu$  is used to correct the data, while *f*'' and *f*' are used to correct the model. Therefore, the true value of  $\mu$  could potentially be found by repeatedly refining *f*'' and then applying the resulting  $\mu$  to the absorption correction until convergence is reached.

Using the respective charged atomic form factors for uranium (U<sup>4+</sup> for the fluorides and U<sup>6+</sup> for the titanates) showed only a little deviation from the values obtained by using the neutral uranium atomic form factor. While the fluorides showed no significant difference, the *f*' obtained using charged uranium for the titanates did show lower absolute values than when using the neutral atomic form factor. This is consistent with the higher charge at the U<sup>6+</sup> ion in the uranyl titanate structures. Again, the difference in *f*' and *f*'' for the two uranium positions in Cs<sub>2</sub>(UO<sub>2</sub>)Ti<sub>2</sub>O<sub>6</sub> was only marginal.

As the structures of the four compounds in our study had previously been determined using Mo K $\alpha$  radiation, we applied ADR to these previously published datasets.<sup>18,20</sup> Figure 4 shows the residual electron density maps of NaUF<sub>5</sub> with and without refined anomalous dispersion correction parameters. This map describes the observed electron density, which could not be completely described by the crystallographic model. Therefore, we attributed the significant reduction of this density to the improved correction by ADR for the nonelastic behavior. Even though the published structure was already of high quality, ADR improved the agreement of observed and modeled intensities even more. Subsequently, both the maximum and the minimum residual electron density peaks decreased. Table 1 shows the respective improvements for all four compounds with their corresponding values for the anomalous dispersion correction.

Generally, ADR improved the crystallographic model, resulting in better quality parameters, lower residuals, as well as lower weights on both the low- and high-resolution reflections. The deviation from the tabulated anomalous dispersion parameters according to Brennan and Cowan<sup>30</sup> (-9.7 e, 9.7 e) was rather large. The values by Brennan and Cowan<sup>30</sup> differ more strongly from those of Sasaki<sup>34</sup> (-11.0 e, 9.7 e) and Henke et al.<sup>19</sup> (-10.2 e, 10.4 e). In particular, *f*'' reached higher values in the free refinement than all tabulated sources, especially prominent for NaUF<sub>5</sub> with a value of 11.8 e.

Remeasurement of the crystals subject to this study on an in-house diffractometer (Rigaku XtaLAB Synergy-DW, HyPix-Arc 150°) generally showed good agreement compared to the published structures. Further information can be found in the SI.

We are therefore confident in recommending ADR for uranium structures measured using in-house diffractometers and Mo K $\alpha$  radiation. However, this method should only be applied to high-quality datasets, without unresolved other issues, such as disorder, twinning, or anharmonicity. The warnings implemented in *Olex2* should always be carefully considered if the values resulting from the ADR differ significantly from tabulated values.

## CONCLUSIONS

In this work, we demonstrated the ability to perform anomalous dispersion refinements for very heavy elements in the energy range of their L absorption edges using four different uranium compounds as examples. The ADR's *f*'' and *f*' followed the independently recorded X-ray absorption spectra and Kramers–Kronig transformation closely, even in the delicate edge region. In the case of Cs<sub>2</sub>(UO<sub>2</sub>)Ti<sub>2</sub>O<sub>6</sub>, which contains two crystallographically independent but chemically identical uranium positions, the deviation of *f*' and *f*'' for both positions was negligible. This underlines the benefit of refining individual dispersion parameters for spatially and chemically different elements. We have also shown that treatment of the anomalous dispersion as a free parameter leads to an improvement in the structural models of measurements with the laboratory diffractometer far away from the absorption edges. The published structures of the four compounds subject to this study, measured at an in-house diffractometer using common Mo K $\alpha$  radiation, could be improved by applying ADR.

## ASSOCIATED CONTENT

### Supporting Information

The Supporting Information is available free of charge at <https://pubs.acs.org/doi/10.1021/acs.inorgchem.4c01772>.

Descriptions of synthetic, crystallographic, and spectroscopic data (PDF)

The starting models for each of the four compounds are attached as a crystallographic information file (".cif"); all results of the ADR procedure including the unedited.cifs as well as the tabulated results are given in ASM1 and ASM2; crystal structures using charged atomic form factors are given in ASM3; the details of the synthetic procedures and data processing as well as further



crystallographic details; ASM1—containing tabulates results from the ADR procedure (.zip, containing.csv); ASM2—crystal structures from the ADR procedure (.zip, containing.cif); ASM3—crystal structures of charged atomic form factors (.zip, containing.cif) (ZIP)

### Accession Codes

CCDC 2337500, 2337534, 2337544, and 2337547 contain the supporting crystallographic data for this paper. These data can be obtained free of charge via [www.ccdc.cam.ac.uk/data\\_request/cif](http://www.ccdc.cam.ac.uk/data_request/cif) or by emailing [data\\_request@ccdc.cam.ac.uk](mailto:data_request@ccdc.cam.ac.uk), or by contacting The Cambridge Crystallographic Data Centre, 12 Union Road, Cambridge CB2 1EZ, UK; fax: +44 1223 336033.

### AUTHOR INFORMATION

#### Corresponding Authors

**Christoph Hennig** – Institute of Resource Ecology, Helmholtz-Zentrum Dresden-Rossendorf (HZDR), Dresden 01314, Germany; Rossendorf Beamline (BM20-CRG), European Synchrotron Radiation Facility (ESRF), Grenoble 38043, France; [orcid.org/0000-0001-6393-2778](https://orcid.org/0000-0001-6393-2778); Email: [hennig@esrf.fr](mailto:hennig@esrf.fr)

**Michael Bodensteiner** – Faculty for Chemistry and Pharmacy, University of Regensburg, Regensburg 93053, Germany; [orcid.org/0000-0002-1850-5192](https://orcid.org/0000-0002-1850-5192); Email: [michael.bodensteiner@ur.de](mailto:michael.bodensteiner@ur.de)

#### Authors

**Florian Meurer** – Faculty for Chemistry and Pharmacy, University of Regensburg, Regensburg 93053, Germany; Institute of Resource Ecology, Helmholtz-Zentrum Dresden-Rossendorf (HZDR), Dresden 01314, Germany; [orcid.org/0000-0002-5689-5451](https://orcid.org/0000-0002-5689-5451)

**Gregory Morrison** – Department of Chemistry and Biochemistry, University of South Carolina, Columbia, South Carolina 29208, United States; [orcid.org/0000-0001-9674-9224](https://orcid.org/0000-0001-9674-9224)

**Birgit Hischa** – Faculty for Chemistry and Pharmacy, University of Regensburg, Regensburg 93053, Germany

**Hans-Conrad zur Loye** – Department of Chemistry and Biochemistry, University of South Carolina, Columbia, South Carolina 29208, United States; [orcid.org/0000-0001-7351-9098](https://orcid.org/0000-0001-7351-9098)

Complete contact information is available at: <https://pubs.acs.org/10.1021/acs.inorgchem.4c01772>

#### Author Contributions

The manuscript was written through the contributions of all authors. All authors have approved the final version of the manuscript.

#### Funding

This work was supported by the Bundesministerium für Bildung und Forschung (BMBF) AcE grant (02NUK060). We acknowledge the HZDR BM20 ROBL station at ESRF for providing beamtime in the frame of the AcE project. F.M. is grateful to the Studienstiftung des Deutschen Volkes for his PhD fellowship. H.-C.z.L. and G.M. acknowledge support from the Center for Hierarchical Waste Form Materials (CHWM), an Energy Frontier Research Center (EFRC) under U.S. Department of Energy (DOE) Award DE-SC0016574.

#### Notes

The authors declare no competing financial interest.

### ACKNOWLEDGMENTS

The authors would like to thank Lisa Uhlstein for her help with the graphical abstract.

### REFERENCES

- (1) Kramers, H. A. La Diffusion de La Lumiere Par Les Atomes. *Atti Cong. Intern. Fisica* **1927**, *2*, 545–557.
- (2) de L. Kronig, R. On the Theory of Dispersion of X-Rays. *J. Opt. Soc. Am.* **1926**, *12* (6), 547.
- (3) Einsle, O.; Andrade, S. L. A.; Dobbek, H.; Meyer, J.; Rees, D. C. Assignment of Individual Metal Redox States in a Metalloprotein by Crystallographic Refinement at Multiple X-Ray Wavelengths. *J. Am. Chem. Soc.* **2007**, *129* (8), 2210–2211.
- (4) Rohde, M.; Grunau, K.; Einsle, O. CO Binding to the FeV Cofactor of CO-Reducing Vanadium Nitrogenase at Atomic Resolution. *Angew. Chem., Int. Ed.* **2020**, *59* (52), 23626–23630.
- (5) Spatzal, T.; Schlesier, J.; Burger, E.-M.; Sippel, D.; Zhang, L.; Andrade, S. L. A.; Rees, D. C.; Einsle, O. Nitrogenase FeMoco Investigated by Spatially Resolved Anomalous Dispersion Refinement. *Nat. Commun.* **2016**, *7* (1), No. 10902.
- (6) Bartholomew, A. K.; Musgrave, R. A.; Anderton, K. J.; Juda, C. E.; Dong, Y.; Bu, W.; Wang, S.-Y.; Chen, Y.-S.; Betley, T. A. Revealing Redox Isomerism in Trichromium Imides by Anomalous Diffraction. *Chem. Sci.* **2021**, *12* (47), 15739–15749.
- (7) Bartholomew, A. K.; Teesdale, J. J.; Hernández Sánchez, R.; Malbrecht, B. J.; Juda, C. E.; Ménard, G.; Bu, W.; Iovan, D. A.; Mikhailine, A. A.; Zheng, S.-L.; Sarangi, R.; Wang, S. G.; Chen, Y.-S.; Betley, T. A. Exposing the Inadequacy of Redox Formalisms by Resolving Redox Inequivalence within Isovalent Clusters. *Proc. Natl. Acad. Sci. U.S.A.* **2019**, *116* (32), 15836–15841.
- (8) Templeton, L. K.; Templeton, D. H. Cesium Hydrogen Tartrate and Anomalous Dispersion of Cesium. *Acta Crystallogr., Sect. A: Cryst. Phys., Diffr., Theor. Gen. Crystallogr.* **1978**, *34* (3), 368–371.
- (9) Templeton, D. H.; Templeton, L. K.; Phillips, J. C.; Hodgson, K. O. Anomalous Scattering of X-Rays by Cesium and Cobalt Measured with Synchrotron Radiation. *Acta Crystallogr., Sect. A: Cryst. Phys., Diffr., Theor. Gen. Crystallogr.* **1980**, *36* (3), 436–442.
- (10) Meurer, F.; Dolomanov, O. V.; Hennig, C.; Peyerimhoff, N.; Kleemiss, F.; Puschmann, H.; Bodensteiner, M. Refinement of Anomalous Dispersion Correction Parameters in Single-Crystal Structure Determinations. *IUCr* **2022**, *9* (5), 604–609.
- (11) Leinders, G.; Grendal, O. G.; Arts, I.; Bes, R.; Prozhnev, I.; Orlat, S.; Fitch, A.; Kvashnina, K.; Verwerft, M. Refinement of the Uranium Dispersion Corrections from Anomalous Diffraction. *J. Appl. Crystallogr.* **2024**, *57* (2), 284.
- (12) zur Loye, H.-C.; Besmann, T.; Amoroso, J.; Brinkman, K.; Grandjean, A.; Henager, C. H.; Hu, S.; Mixture, S. T.; Phillipot, S. R.; Shustova, N. B.; Wang, H.; Koch, R. J.; Morrison, G.; Dolgoplova, E. Hierarchical Materials as Tailored Nuclear Waste Forms: A Perspective. *Chem. Mater.* **2018**, *30* (14), 4475–4488.
- (13) Burns, P. C.; Ewing, R. C.; Hawthorne, F. C. The Crystal Chemistry of Hexavalent Uranium: Polyhedron Geometries, Bond-Valence Parameters, and Polymerization of Polyhedra. *Can. Mineral.* **1997**, *35*, 1551–1570.
- (14) Severance, R. C.; Smith, M. D.; zur Loye, H.-C. Three-Dimensional Hybrid Framework Containing U<sub>2</sub>O<sub>13</sub> Dimers Connected via Cation–Cation Interactions. *Inorg. Chem.* **2011**, *50* (17), 7931–7933.
- (15) Balboni, E.; Burns, P. C. Cation–Cation Interactions and Cation Exchange in a Series of Isostructural Framework Uranyl Tungstates. *J. Solid State Chem.* **2014**, *213*, 1–8.
- (16) Read, C. M.; Yeon, J.; Smith, M. D.; Loye, H.-C. zur. Crystal Growth, Structural Characterization, Cation–Cation Interaction Classification, and Optical Properties of Uranium(VI) Containing Oxochlorides, A<sub>4</sub>U<sub>5</sub>O<sub>16</sub>Cl<sub>2</sub> (A = K, Rb), Cs<sub>5</sub>U<sub>7</sub>O<sub>22</sub>Cl<sub>3</sub>, and AUO<sub>3</sub>Cl (A = Rb, Cs). *CrystEngComm* **2014**, *16* (31), 7259–7267.
- (17) Yeon, J.; Smith, M. D.; Tapp, J.; Möller, A.; zur Loye, H.-C. Application of a Mild Hydrothermal Approach Containing an in Situ

Reduction Step to the Growth of Single Crystals of the Quaternary U(IV)-Containing Fluorides Na<sub>4</sub>MU<sub>6</sub>F<sub>30</sub> (M = Mn<sup>2+</sup>, Co<sup>2+</sup>, Ni<sup>2+</sup>, Cu<sup>2+</sup>, and Zn<sup>2+</sup>) Crystal Growth, Structures, and Magnetic Properties. *J. Am. Chem. Soc.* **2014**, *136* (10), 3955–3963.

(18) Klepov, V. V.; Felder, J. B.; zur Loye, H.-C. Synthetic Strategies for the Synthesis of Ternary Uranium(IV) and Thorium(IV) Fluorides. *Inorg. Chem.* **2018**, *57* (9), 5597–5606.

(19) Henke, B. L.; Lee, P.; Tanaka, T. J.; Shimabukuro, R. L.; Fujikawa, B. K. Low-Energy x-Ray Interaction Coefficients: Photoabsorption, Scattering, and Reflection: E = 100–2000 eV Z = 1–94. *At. Data Nucl. Data Tables* **1982**, *27* (1), 1–144.

(20) Morrison, G.; Christian, M. S.; Besmann, T. M.; zur Loye, H.-C. Flux Growth of Uranyl Titanates: Rare Examples of TiO<sub>4</sub> Tetrahedra and TiO<sub>5</sub> Square Bipyramids. *J. Phys. Chem. A* **2020**, *124* (45), 9487–9495.

(21) Uranium. [https://xdb.lbl.gov/Section1/Periodic\\_Table/U\\_Web\\_data.htm](https://xdb.lbl.gov/Section1/Periodic_Table/U_Web_data.htm) (accessed Feb 14, 2024).

(22) Scheinost, A. C.; Claussner, J.; Exner, J.; Feig, M.; Findeisen, S.; Hennig, C.; Kvashnina, K. O.; Naudet, D.; Prieur, D.; Rossberg, A.; Schmidt, M.; Qiu, C.; Colomp, P.; Cohen, C.; Dettona, E.; Dyadkin, V.; Stumpf, T. ROBL-II at ESRF: A Synchrotron Toolbox for Actinide Research. *J. Synchrotron Radiat.* **2021**, *28* (1), 333–349.

(23) *Crystalis PRO*; Rigaku Oxford Diffraction Ltd., 2019.

(24) Dolomanov, O. V.; Bourhis, L. J.; Gildea, R. J.; Howard, J. A. K.; Puschmann, H. OLEX2: A Complete Structure Solution, Refinement and Analysis Program. *J. Appl. Crystallogr.* **2009**, *42* (2), 339–341.

(25) Bourhis, L. J.; Dolomanov, O. V.; Gildea, R. J.; Howard, J. A. K.; Puschmann, H. The Anatomy of a Comprehensive Constrained, Restrained Refinement Program for the Modern Computing Environment – Olex2 Dissected. *Acta Crystallogr., Sect. A: Found. Adv.* **2015**, *71* (1), 59–75.

(26) GitHub - FlorianMeurer/plugin-SISYPHOS: SISYPHOS software for the serial modelling of crystallographic data for the same structure within Olex2. <https://github.com/FlorianMeurer/plugin-SISYPHOS> (accessed April 05, 2024).

(27) Blessing, R. H. An Empirical Correction for Absorption Anisotropy. *Acta Crystallogr., Sect. A: Found. Crystallogr.* **1995**, *51* (1), 33–38.

(28) Solé, V.; Papillon, E.; Cotte, M.; Walter, P.; Susini, J. A Multiplatform Code for the Analysis of Energy-Dispersive X-Ray Fluorescence Spectra. *Spectrochim. Acta, Part B* **2007**, *62* (1), 63–68.

(29) Watts, B. Calculation of the Kramers-Kronig Transform of X-Ray Spectra by a Piecewise Laurent Polynomial Method. *Opt. Express* **2014**, *22* (19), 23628–23639.

(30) Brennan, S.; Cowan, P. L. A Suite of Programs for Calculating X-Ray Absorption, Reflection, and Diffraction Performance for a Variety of Materials at Arbitrary Wavelengths. *Rev. Sci. Instrum.* **1992**, *63* (1), 850–853.

(31) Gianopoulos, C. G.; Zhurov, V. V.; Minasian, S. G.; Batista, E. R.; Jelsch, C.; Pinkerton, A. A. Bonding in Uranium(V) Hexafluoride Based on the Experimental Electron Density Distribution Measured at 20 K. *Inorg. Chem.* **2017**, *56* (4), 1775–1778.

(32) Koga, T.; Kanayama, K.; Watanabe, T.; Imai, T.; Thakkar, A. J. Analytical Hartree–Fock Wave Functions for the Atoms Cs to Lr. *Theor. Chem. Acc.* **2000**, *104* (5), 411–413.

(33) Kleemiss, F.; Peyerimhoff, N.; Bodensteiner, M. Refinement of X-Ray and Electron Diffraction Crystal Structures Using Analytical Fourier Transforms of Slater-Type Atomic Wavefunctions in Olex2. *J. Appl. Crystallogr.* **2024**, *57* (1), 161–174.

(34) Sasaki, S. *Numerical Tables of Anomalous Scattering Factors Calculated by the Cromer and Liberman's Method*; Japan, 1989; p 137.